Extended Abstracts of the 2004 International Conference on Solid State Devices and Materials, Tokyo, 2004, pp. 926-927

H-8-4

Simulation of Ultrafast Intersubband Optical Modulation Achieved in GaN/AlN Ridge Waveguide

Nobuo Suzuki, Norio Iizuka and Kei Kaneko

Corporate Research & Development Center, Toshiba Corporation
1, Komukai-Toshiba-cho, Saiwai-ku, Kawasaki, Kanagawa 212-8582, Japan
Phone: +81-44-549-2141, Fax: +81-44-520-1501, E-mail: nob.suzuki@toshiba.co.jp

1. Introduction

The saturation of intersubband absorption in semiconductor multiple quantum wells (MQWs) is an attractive mechanism for ultrafast (>100 Gb/s) all-optical switches because of ultrafast recovery (~1 ps) [1]. Recovery times of the intersubband transitions (ISBTs) in the optical communication wavelength range have been reported in InGaAs/AlAsSb coupled-QWs (690 fs) [2], CdS/ZnSe/BeTe MQWs (190 fs) [3], and GaN/Al(Ga)N MQWs (140-400 fs) [4]-[6]. Faster intersubband relaxations in GaN and II-VI semiconductors are due to strong interaction between electrons and LO-phonons [7],[8]. In addition to the ultrafast response, GaN has many advantages. Since the homogeneous spectral linewidth is broad (~100 meV), a wide range (~200 nm) of the wavelength is available. It is suitable for high-power, high-temperature operation. Since the band gap is wide, two-photon absorption (TPA) does not interfere with the saturable absorption (SA).

Simulation by a one-dimensional finite-difference time-domain (FDTD) model [9],[10] has suggested that GaN/AlGaN optical waveguide switches will function even at 1 Tb/s without a serious pattern effect. Recently, we have achieved ultrafast optical modulation due to the saturation of intersubband absorption in a GaN/AlN ridge waveguide for the first time (Details will be presented elsewhere.). In this paper, the measured characteristics are compared with those calculated by the FDTD model. The experimental data were satisfactorily explained by the simulation.

2. Device Structure

The ridge waveguide was fabricated using molecular beam epitaxy (MBE) and Cl_2-based electron cyclotron resonance reactive ion beam etching (ECR-RIBE). The sample structure is schematically shown in Fig. 1. Multiple intermediate layers (MIL) consisting of 10 pairs of undoped GaN (40 nm) and AlN (10 nm) were inserted to reduce the dislocation density. The MQW consists of 10 pairs of *n*-GaN wells (2 nm) and AlN barriers (3 nm). The wells were doped with Si by 5×10^{19} cm^{-3}. The peak wavelength and the full width at half maximum (FWHM) of the intersubband absorption spectrum were designed to be 1.62 μm and 160 meV, respectively. The thicknesses of upper and lower GaN layers were 960 nm and 480 nm, respectively. The device length was 400 μm. The width of mesa was 1 μm, but it was tapered to 2 μm near the cleaved facet. It was antireflection-coated and housed in a module with polarization-maintaining fiber pig tails.

The ISBT occurs only for TM polarization. At 1.55 μm, the fiber-to-fiber insertion loss for TE-polarized pulses was 8.1 dB independent of the input pulse energy. For TM mode, the loss before the saturation was 34.8 dB. The polarization dependent loss (PDL) is caused not only by the ISBT. We have found that some of the carriers are trapped by edge dislocations. This causes an excess background loss for TM-mode [11] and reduces the carrier density in the wells. The optical characteristics were evaluated using optical pulses (λ = 1.55 μm and 1.7 μm) generated by an optical parametric oscillator (OPO), which was excited by a Ti:sapphire laser.

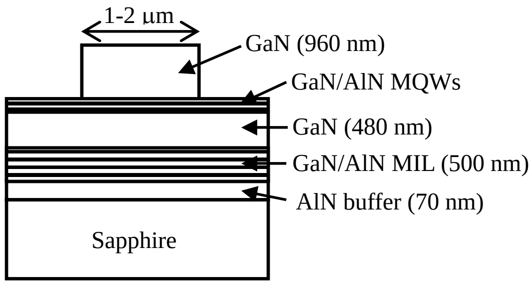

Fig. 1 Structure of the fabricated GaN/AlN ridge waveguide.

3. FDTD Simulation

The characteristics of the waveguide have been calculated by a one-dimensional FDTD model, where the intersubband carrier dynamics were incorporated by rate equations [10]. The intersubband relaxation time and the homogeneous line width were assumed to be 110 fs and 100 meV, respectively [7],[8]. In the idealized ridge waveguide, the switching energy required for a 10-dB extinction ratio was calculated to be about 10 pJ. However, the characteristics of actual devices are affected by the inhomogeneous broadening, the background absorption, and the mode field profile in the MQW. Here, these extrinsic effects were taken into consideration. The inhomogeneous spectral line width was assumed to be 158 meV. The carrier concentration in the well was assumed to be 50% of the donor density, based on the data for the MQW samples with large numbers of wells [12]. The TM excess loss was assumed to be 10 dB. From the device length dependency of the insertion loss, the background loss for the TE mode and the coupling loss were assumed to be 2 dB and 3 dB/facet, respectively. The ratio of the effective field in the MQWs to the peak of the mode profile was utilized as a fitting parameter.

4. Saturation Characteristics

Fig. 2 shows the pulse energy dependency of the fiber-to-fiber insertion loss for 1.55-μm, 130-fs TM-mode pulses. The circles and the solid line show the measured and the calculated results, respectively. The loss before the saturation fit to the measured one when the effective field strength in the MQWs was assumed to be 40% of the peak. The calculation is in good agreement with the measured data, although the saturation is slightly stronger.

The characteristics of the sample were suffered from the extrinsic effects, especially from the excess TM loss. The dashed line shows the calculated characteristics without the 10-dB excess loss. Reduction of the dislocation density is important to improve the insertion loss, the switching energy, and the extinction ratio. For further reduction of the switching energy, waveguides with a smaller cross section are required. In that case, spot size converters should be integrated to reduce the coupling loss.

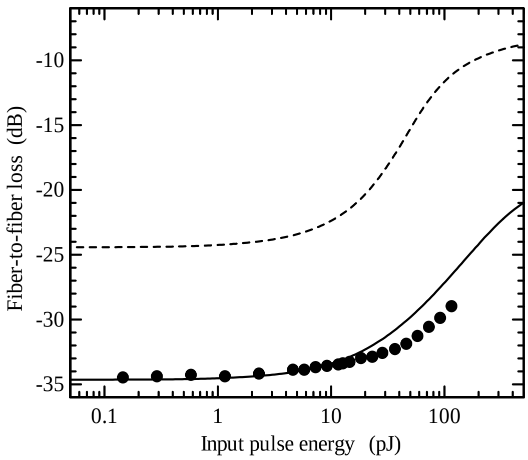

Fig. 2 Input pulse energy dependence of the insertion loss for TM mode at λ =1.55 μm. The solid circles and the solid line show the measured and calculated data. The dashed line shows the characteristics without the excess TM loss.

5. Ultrafast Optical Modulation

Fig. 3 (a) shows the measured change in the transmittance for 1.55-μm, 130-fs, 10-pJ probe pulses caused by 1.7-μm, 230-fs, 120-pJ pump pulses. The transmittance changed only when both the pump and the probe pulses were TM-polarized. The on/off ratio was 2.5 dB. The gate window (FWHM) was 360 fs, and the time constant for the absorption recovery was 185 fs. As well as the ultrafast recovery, the broad homogeneous line width of the ISBT in GaN was verified by the fact that the 1.55-μm probe light was instantaneously modulated by the 1.7-μm pump light.

Fig. 3 (b) shows the calculated results. The intrasubband relaxation time (including the time for carrier cooling) was assumed to be τ_{intra} = 100 fs (dotted line) and 300 fs (solid line). The latter fit the measured data. These results suggest that the GaN/AlN ISBT switches will operate at 1 Tb/s without a serious pattern effect.

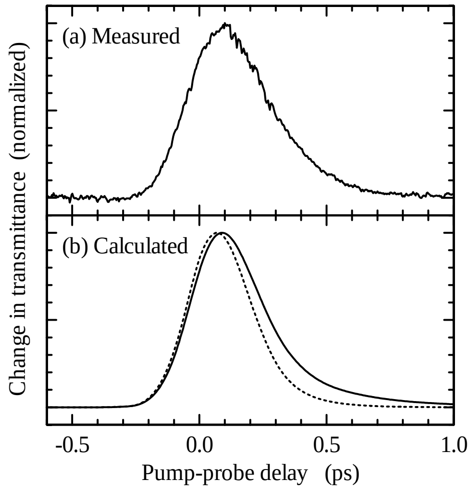

Fig. 3 Change in transmittance for 1.55-μm, 10-pJ, 150-fs probe pulses due to 1.7-μm, 120-pJ, 230-fs control pulses. (a) Measured response. (b) Calculated results for τ_{intra} = 100 fs (dotted line) and 300 fs (solid line).

6. Conclusions

The ultrafast optical modulation due to the saturation of the intersubband absorption in a GaN/AlN ridge waveguide has been simulated by a one-dimensional FDTD model, in which the inhomogeneous broadening, the field profile in the MQWs, and the excess loss were taken into consideration. The results were in good accordance with the experimental data, and suggested that the 1-Tb/s switching operation will be possible. Saturation characteristics will be improved by the reduction of dislocation density.

Acknowledgements

This work was performed under the supervision of The Femtosecond Technology Research Association (FESTA), which is supported by New Energy and Industrial Technology Development Organization (NEDO).

References

[1] S. Noda *et al.*, J. Appl. Phys. **68** (1990) 6529.
[2] T. Akiyama *et al.*, Electron. Lett. **37** (2001) 129.
[3] R. Akimoto *et al.*, Appl. Phys. Lett. **81** (2002) 2998.
[4] J. D. Heber *et al.*, Appl. Phys. Lett. **81** (2002) 1237.
[5] N. Iizuka *et al*., Appl. Phys. Lett. **81** (2002) 1803.
[6] J. Hamazaki *et al*., Appl. Phys. Lett. **84** (2004) 1102.
[7] N. Suzuki and N. Iizuka, Jpn. J. Appl. Phys. **36** (1997) L1006.
[8] N. Suzuki and N. Iizuka, Jpn. J. Appl. Phys. **37** (1998) L369.
[9] N. Suzuki, Opt. Quantum Electron. **33** (2001) 985.
[10] N. Suzuki, *et al.*, IEICE Trans. Electron. **E83-C** (2000) 981.
[11] N. Iizuka, *et al.*, *Extended Abstracts of the 51st Spring Meeting, 2004, the Japan Society of Applied Physics and Related Societies,* No.3, 30a-ZV-6, p.1306 (in Japanese).
[12] N. Suzuki, *et al.*, Jpn. J. Appl. Phys. **42** (2003) 132.